Acknowledgment. This work was part of the M.S. Thesis Research of H. Z. (1988), San Francisco State University. It was supported by NIH Grant DK-31038 (F.A.W.) and by the NIH (RR 02684) and the NSF (DMB-8516065) for purchase of the NMR spectrometer.

Fused Iron Catalyzed Conversion of Benzene to Toluene

S. Mark Davis* and Carl W. Hudson

Exxon Research and Development Laboratory
P.O. Box 2226, Baton Rouge, Louisiana 70821

Received April 12, 1990

Whereas benzene hydrogenation catalyzed over group VIII metals has been investigated, intensively,[1,2] very few reports[3] have considered ring hydrogenolysis of this simple aromatic hydrocarbon. We have recently discovered that *surface carbon reincorporation* to produce toluene and xylenes (reaction IA) is an important reaction operating during benzene hydrogenolysis (reaction IB) over a conventional fused iron ammonia synthesis catalyst. Intrinsic selectivity for the novel reaction IA is substantial over a wide range of temperatures; however, synthetic utility is limited by secondary reactions involving preferential conversion of alkylbenzenes. Benzene conversion is accompanied by carbiding of the catalyst near surface region.

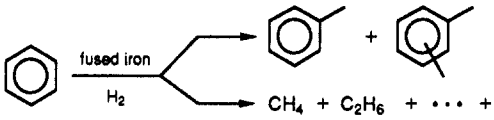

(IA)

(IB)

Reaction studies were carried out at atmospheric pressure in an apparatus equipped with a microflow reactor and a surface analysis system with capabilities for X-ray photoemission (XPS) and low energy helium ion scattering (LEIS).[4] Research grade H_2 was used as supplied, whereas benzene (MCB, "thiophene-free") was filtered over activated alumina, freeze–pumped, and purged with dry H_2 before use. The BASF-R catalyst exhibited a nominal composition (wt %) of 2–3% Al_2O_3, 0.6–1.0% K_2O, 1.0–1.5% CaO, and 95% free iron. Catalysts were activated by H_2 treatment at 490–500 °C for 1 h, an XPS spectrum was recorded, and the catalyst was returned to the reactor. After 0.5–15 h of reaction time, the catalyst was cooled to 70 °C before evacuation of the gas mixture and recording of another XPS spectrum. Subsequently, the reactivity of carbon deposits was explored by using temperature-programmed hydrogen treatment (TPHT) wherein the catalyst was heated in flowing H_2 at a rate of 5 K/min, and the evolution of hydrocarbons was detected with a gas chromatograph.

Initial rates and product distributions for benzene conversion at 280–380 °C and at several conversion levels are compared in Table I. Toluene and methane were major products along with small yields of C_2–C_5 alkanes and xylenes in an approximate 1:2 ratio for the para:meta:ortho isomers. Consistent with earlier work,[1a,c] hydrogenation to cyclohexane could not be detected. After an initial 1–2-h period of increasing catalytic activity, rates for all reactions gradually declined over many hours.[5]

Table I. Rates and Product Distributions for Benzene Conversion over BASF Fused Iron[a]

reactn T, °C	reactn rate, molecules/(gr s)	benzene conversn, %	product distributn, wt %			
			toluene	xylenes	CH_4	C_2–C_5
280	9.2×10^{16}	0.4	60		36	4.4
350	1.0×10^{18}	1.3	65	3.2	31	1.5
350		16	34	1.0	60	4.8
350		25	26	1.3	68	5.1
380	2.0×10^{18}	1.9	64	3.0	32	1.3

[a] At 1 atm, H_2/Bz = 8 (molar ratio).

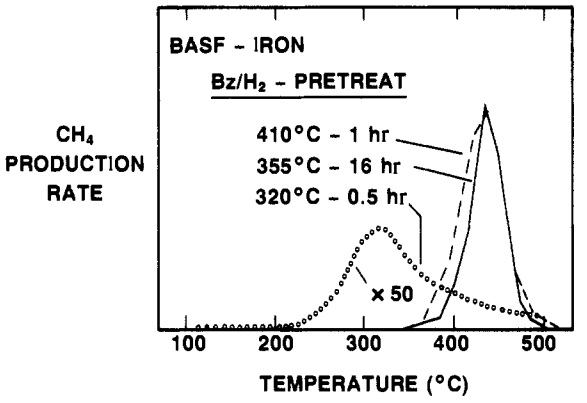

Figure 1. TPHT profiles illustrating hydrogenation of carbonaceous species produced during benzene conversion over a fused iron ammonia synthesis catalyst.

For benzene conversion levels below 3%, conversion-dependent changes in selectivity were not detected. However, at higher conversions (cf. Table I), selectivity for toluene and xylene production decreased sharply, indicating preferential conversion by secondary hydrogenolysis reactions. Despite this limitation, it is apparent that fused iron displayed unusual selectivity for carbon incorporation.

The hydrogenolysis product distributions suggest a reaction pathway where ring opening is followed by scission of essentially all C–C bonds before rehydrogenation. Reaction of the intermediate CH_x surface species with an adsorbed benzene derivative produces toluene, whereas complete hydrogenation produces methane. Considering the relative rates of toluene and light alkane production, the probability for carbon reincorporation (rather than hydrogenation to methane) appears to be 0.2–0.3.

The carbon incorporation reaction occurred with extraordinary selectivity for a metal-catalyzed reaction of this type. Previous reports[6] have noted heavier hydrocarbons during alkane hydrogenolysis over Co and Ru, although selectivities for carbon incorporation were only 1–5%. Eckerdt and Bell et al.[7] have also reported reactive scavenging of CH_x species with cyclohexene and pyridine during Fischer–Tropsch (FT) synthesis over Ru and Fe/SiO_2. Our studies confirm that CH_x species are active for reincorporation over a wide range of temperatures exceeding those normally applied in FT synthesis. A common feature of these reactions is their occurrence over FT-active metals implying that similar intermediates participate in both reactions.

Photoemission results showed that iron was well reduced after H_2 activation and remained well reduced after reaction studies. In agreement with earlier work,[8] XPS, LEIS, and CO-chemi-

(1) (a) Yoon, K. J.; Vannice, M. A. *J. Catal.* **1983**, *82*, 457. (b) Yoon, K. J.; Mulay, L. W.; Walker, P. L.; Vannice, M. A. *Ind. Eng. Chem. Prod. Res. Dev.* **1983**, *22*, 519. (c) Norval, G. W.; Phillips, M. J. *J. Catal.* **1989**, *115*, 250. (d) Chou, P.; Vannice, M. A. *J. Catal.* **1987**, *107*, 129. (e) van Meerten, R. Z. C.; Morales, A.; Barbier, J.; Maurel, R. *J. Catal.* **1979**, *58*, 43.

(2) For reviews, see: (a) Davis, S. M.; Somorjai, G. A. In *The Chemical Physics of Solid Surfaces and Heterogeneous Catalysis*; King, D. A., Woodruff, D. P., Eds.; Elsevier: Amsterdam, 1982; Vol. 4, p 217. (b) Peterson, R. J. *Hydrogenation Catalysts*; Noyes Data Corp.: Park Ridge, NJ, 1977; p 129. (c) Anderson, J. R.; Kemball, C. In *Advances in Catalysis*; Eley, D. D., Farkas, A., Eds.; Academic Press: San Diego, 1957; Vol. 9, p 51.

(3) (a) Kubicka, H. *J. Catal.* **1968**, *12*, 223. (b) Freel, J.; Galwey, A. K. *J. Catal.* **1968**, *10*, 277. (c) Phillips, M. J.; Emmett, P. H. *J. Catal.* **1986**, *101*, 268.

(4) (a) Davis, S. M.; Somorjai, G. A. *Bull. Soc. Chim. Fr.* **1985**, 271. (b) Dwyer, D. J. In *Catalyst Characterization Science*; Deviney, M. L., Gland, J. L., Eds.; ACS Symposium Series 288; American Chemical Society: Washington, DC, 1986.

(5) Davis, S. M.; Hudson, C. W., to be published.

(6) (a) Osterloh, W. T.; Cornell, M. E.; Petit, R. *J. Am. Chem. Soc.* **1982**, *104*, 3759. (b) Donahue, C. O.; Clarke, J. K. A.; Rooney, J. *J. Chem. Soc., Faraday Trans. 1* **1980**, *76*, 345.

(7) (a) Eckerdt, J. G.; Bell, A. T. *J. Catal.* **1980**, *62*, 19. (b) Eckerdt, J. G.; Wang, C. J. *J. Catal.* **1983**, *80*, 172. (c) Eckerdt, J. G.; Wang, C. J. *J. Catal.* **1984**, *86*, 239. (d) Anderson, K. G.; Eckerdt, J. G. *J. Catal.* **1985**, *95*, 423.

0002-7863/90/1512-6126$02.50/0

sorption results[9] revealed that the iron surface was mostly covered by promoter oxides of Al, Ca, and K. Postreaction XPS results also revealed a C(1s) XPS peak of weak to moderate intensity centered at 284.1-283.7 eV. This binding energy approaches those (ca. 283.5 eV) reported for iron carbides.[4b,10]

More convincing evidence for carbide formation was obtained from TPHT results collected after reaction studies like those displayed in Figure 1 in which methane was the only product. After reaction at temperatures below 340 °C, only small amounts of reactive carbon could be distinguished with maximum methane desorption rates near 300 °C. However, for higher reaction temperatures, large amounts of methane were produced with a maximum rate just above 400 °C. Since XPS results revealed only small amounts of carbonaceous residue on top of the catalyst surface, this reactive carbon must be associated with carbiding of the catalyst. Consequently, it appears that the active carbon incorporation catalyst is carbided iron. This conclusion is well supported by bulk carbon to iron stoichiometries of 0.1-0.25 estimated from the TPHT peak areas which were adequate to represent 40-60% conversion to bulk carbides such as Fe_3C or Fe_5C_2. Moreover, preliminary results from studies using bona fide iron carbides have shown similar catalytic behavior.[5]

Acknowledgment. We acknowledge contributions by Mr. W. S. Varnado along with support of this research by the Exxon Research and Engineering Company.

(8) (a) Silverman, D. C.; Boudart, M. *J. Catal.* **1982**, *77*, 208. (b) Ertl, G.; Thiele, N. *Appl. Surf. Sci.* **1979**, *3*, 99. (c) Brunauer, S.; Emmett, P. H. *J. Am. Chem. Soc.* **1940**, *62*, 1732.
(9) Davis, S. M. *Catal. Lett.* **1988**, *1*, 85.
(10) (a) Dwyer, D. J.; Hardenbergh, J. H. *J. Catal.* **1984**, *87*, 66. (b) Bonzel, H. P.; Broden, G.; Krebs, H. J. *Appl. Surf. Sci.* **1983**, *16*, 373. (c) Bonzel, H. P.; Krebs, H. J. *Surf. Sci.* **1983**, *109*, L527.

Semianalytical Treatment of Solvation for Molecular Mechanics and Dynamics

W. Clark Still,* Anna Tempczyk, Ronald C. Hawley, and Thomas Hendrickson

Department of Chemistry, Columbia University
New York, New York 10027

Received February 12, 1990

Dealing with solvent has been a perpetual problem for molecular modeling. While using explicit solvent molecules provides one solution to the problem, such calculations require a major computational effort if converged energies are required. Here we describe a more practical alternative in which solvent is treated as a statistical continuum.[1] The treatment provides both energies and derivatives analytically and thus may be used in a molecular mechanics force field. As we will show, it gives small-molecule hydration energies of comparable accuracy to those obtained from contemporary free energy perturbation methods but at only a fraction of the computational expense.

Method. We consider solvation free energy (G_{sol}) traditionally as consisting of a solvent-solvent cavity term (G_{cav}), a solute-solvent van der Waals term (G_{vdW}), and a solute-solvent electrostatic polarization term (G_{pol}):

$$G_{sol} = G_{cav} + G_{vdW} + G_{pol} \quad (1)$$

Noting that G_{sol} for the saturated hydrocarbons in water is linearly related[2] to solvent-accessible surface area (SA), we follow precedent[1a,b] by setting

$$G_{cav} + G_{vdW} = \sum \sigma_k SA_k \quad (2)$$

where SA_k is the total solvent-accessible surface area of atoms of type k and σ_k is an empirical atomic solvation parameter. As a preliminary value for σ_k, we use +7.2 cal/(mol Å^2) for all atom types to reproduce hydration energies of simple hydrocarbons using our recently described analytical surface area calculation.[3]

For G_{pol}, the total electrostatic free energy (G_{es}, kcal/mol) of a system of widely separated particles (separations r (Å), charges q (electrons), radii α (Å)) in a medium of dielectric constant ϵ is given (eq 3) by the sum of Coulomb's law in a dielectric (term 1) and the Born equation (term 2). Term 1 can be expanded algebraically (eq 4) to give Coulomb's law in vacuo and a new second term which accounts for the effect of the dielectric medium on the pairwise interactions of charged particles. The sum of terms 2 and 3 in eq 4 is equal to G_{pol} and has been termed the generalized Born (GB) equation.[4] The similar form of terms 2 and 3 in eq

$$G_{es} = 332\sum_{i=1}^{n-1}\sum_{j=i+1}^{n}\frac{q_iq_j}{r_{ij}\epsilon} - 166\left(1-\frac{1}{\epsilon}\right)\sum_{i}^{n}\frac{q_i^2}{\alpha_i} \quad (3)$$

$$= 332\sum_{i=1}^{n-1}\sum_{j=i+1}^{n}\frac{q_iq_j}{r_{ij}} - 332\left(1-\frac{1}{\epsilon}\right)\sum_{i=1}^{n-1}\sum_{i=i+1}^{n}\frac{q_iq_j}{r_{ij}} - 166\left(1-\frac{1}{\epsilon}\right)\sum_{i}^{n}\frac{q_i^2}{\alpha_i} \quad (4)$$

$$G_{pol} = -166\left(1-\frac{1}{\epsilon}\right)\sum_{i=1}^{n}\sum_{j=1}^{n}\frac{q_iq_j}{f_{GB}} \quad (5)$$

4 prompts us to combine them into a single expression (eq 5) where we define f_{GB} as a function of r_{ij} and α_i which makes eq 5 mimic the relevant equations of classical electrostatics. While we have not defined f_{GB} uniquely, one simple but effective expression is $f_{GB} = (r_{ij}^2 + \alpha_{ij}^2 e^{-D})^{0.5}$ where $\alpha_{ij} = (\alpha_i\alpha_j)^{0.5}$ and $D = r_{ij}^2/(2\alpha_{ij})^2$. Used in eq 5, this expression gives the Born equation for superimposed charges when $r_{ij} = 0$, the Onsager reaction field energy within 10% for a dipole in a spherical cavity when $r_{ij} < 0.1\alpha_{ij}$, and the Born + Coulomb dielectric polarization energy within 1% for two charged spheres when $r_{ij} > 2.5\alpha_{ij}$. It is superior to eq 4, which overestimates the interaction of buried charges with the dielectric, and to $f_{GB} = (r_{ij}^2 + \alpha_{ij}^2)^{0.5}$, which underestimates the corresponding interaction of proximate exposed charges.

We compute Born radii (α_i) numerically for each charged atom i in the solute. This is done by evaluating $G_{pol(i)}$ for each such atom with a continuum dielectric medium using a finite difference method (see supplementary material) assuming that all other atoms are neutral and displace the dielectric. Given $G_{pol(i)}$, the effective spherical Born radius is obtained by solving the Born term of eq 3 ($n = 1$) for α_i. We take the dielectric to begin at some fixed, solvent-dependent distance from the solute van der Waals surface.[5] For water solvent and atomic radii taken from the OPLS force field,[6] we established this dielectric offset empirically as -0.09 Å. We calculate derivatives of eq 5 treating α_i as a constant which can be updated periodically along with the nonbonded pairlist. In the absence of major conformational changes, the simplification of a constant α does not introduce large errors because f_{GB} is ~10 times more sensitive to small changes in r_{ij} than to the associated changes in α_{ij}.

(1) *Numerical* methods of computing G_{sol} or G_{pol} using continuum models: (a) Eisenberg, D.; McLachlan, A. D. *Nature (London)* **1986**, *319*, 199. (b) Ooi, T.; Oobatake, M.; Nemethy, G.; Scheraga, H. A. *Proc. Natl. Acad. Sci. U.S.A.* **1987**, *84*, 3086. (c) Kang, Y. K.; Nemethy, G.; Scheraga, H. A. *J. Phys. Chem.* **1987**, *91*, 4105, 4109, 4118. (d) Warshel, A.; Russel, S. T. *Q. Rev. Biophys.* **1984**, *17*, 283. (e) Gilson, M.; Honig, B. *Proteins* **1988**, *4*, 7.
(2) Hermann, R. B. *J. Phys. Chem.* **1972**, *76*, 2754. Amidon, G. L.; Yalkowsky, S. H.; Anik, S. T.; Valvani, S. C. *J. Phys. Chem.* **1975**, *72*, 2239. See also: Floris, F.; Tomasi, J. *J. Comput. Chem.* **1989**, *10*, 616.
(3) Hasel, W.; Hendrickson, T. F.; Still, W. C. *Tetrahedron Comput. Methodol.* **1988**, *1*, 103.
(4) Constanciel, R.; Contreras, R. *Theor. Chim. Acta* **1984**, *65*, 1. Kozaki, T.; Morihashi, K.; Kikuchi, O. *J. Mol. Struct.* **1988**, *168*, 265. Kozaki, T.; Morihashi, K.; Kikuchi, O. *J. Am. Chem. Soc.* **1989**, *111*, 1547 and references therein. See also: Goodford, P. J. *J. Med. Chem.* **1985**, *28*, 849.
(5) Cf.: Rashin, A. A.; Honig, B. *J. Phys. Chem.* **1985**, *89*, 5588.
(6) Jorgensen, W. L.; Tirado-Rives, J. *J. Am. Chem. Soc.* **1988**, *110*, 1657. For hydrogens bound to heteroatoms, we used the OPLS radius of 0.0 in our FEP calculations whereas we used a radius of 1.15 Å in eq 5. For other atoms, we took 0.5σ as van der Waals radii. We thank Professor Jorgensen for his most recent set of OPLS parameters.

0002-7863/90/1512-6127$02.50/0